

# DOTA–D-Tyr<sup>1</sup>-Octreotate: A Somatostatin Analogue for Labeling with Metal and Halogen Radionuclides for Cancer Imaging and Therapy

Wen Ping Li,<sup>†</sup> Jason S. Lewis,<sup>†</sup> Joonyoung Kim,<sup>†</sup> Joseph E. Bugaj,<sup>‡</sup> Michael A. Johnson,<sup>‡</sup> Jack L. Erion,<sup>‡</sup> and Carolyn J. Anderson<sup>\*,†</sup>

Mallinckrodt Institute of Radiology, Washington University School of Medicine, St. Louis, Missouri 63110 and Mallinckrodt, Inc. 675 McDonnell Blvd., St. Louis, Missouri 63134. Received December 10, 2001; Revised Manuscript Received April 25, 2002

The goal of this study was to evaluate a somatostatin receptor ligand, DOTA–D-Tyr<sup>1</sup>-octreotate (DOTA-DY1-TATE), that has the chelator 1,4,7,10-tetraazacyclotetradecane-*N,N,N',N''*-tetraacetic acid (DOTA) attached to the D-Tyr<sup>1</sup> residue, allowing radiolabeling with both radiohalogens and radiometals. A potential advantage of having a chelator attached to the Tyr<sup>1</sup> residue is that halogen radiolabels may residualize or remain trapped in tumor cells rather than clear from the tumor. DOTA-DY1-TATE was synthesized by solid-phase methods and radiolabeled with <sup>61</sup>Cu, <sup>64</sup>Cu, and <sup>125</sup>I in high radiochemical purity and specific activity. A competitive binding assay demonstrated that <sup>nat</sup>Cu-DOTA-DY1-TATE and DOTA-<sup>nat</sup>I-DY1-TATE had comparable affinity to <sup>nat</sup>In-DTPA-OC in AR42J rat pancreatic tumor cells membranes. <sup>61</sup>Cu-DOTA-DY1-TATE had a dissociation constant (*K<sub>d</sub>*) of 176.4 pM and a receptor concentration (*B<sub>max</sub>*) of 244.4 fmol/mg. A tumor uptake of 1.515 %ID/g was determined for <sup>64</sup>Cu-DOTA-DY1-TATE and 0.814 %ID/g for DOTA-<sup>125</sup>I-DY1-TATE in AR42J tumor bearing Lewis rats at 1 h postinjection. DOTA-<sup>125</sup>I-DY1-TATE remained in the tumor at a higher concentration out to 4 h postinjection, suggesting that the iodine may have residualized in the tumor cells. MicroPET imaging of <sup>64</sup>Cu-DOTA-DY1-TATE in AR42J tumor bearing rats and SCID mice at 2 h postinjection showed significant uptake and good contrast in the thigh tumors in the rat model and in the neck and thigh tumors of the mouse. This study demonstrates that DOTA-DY1-TATE is a somatostatin analogue that can be labeled with both metal and halogen radionuclides, and its <sup>64</sup>Cu- and <sup>125</sup>I-radiolabeled compounds showed somatostatin receptor-mediated uptake in normal and tumor tissues.

## INTRODUCTION

Over the last 15 years, considerable progress has been made in the investigation of radiolabeled somatostatin analogues as radiotherapeutic agents for somatostatin receptor-positive tumors. A number of studies have focused on improving the target tissue uptake of radiolabeled somatostatin analogues. It has been shown that changing the C-terminus from an alcohol to a carboxylic acid increases uptake of the peptide in somatostatin subtype 2 receptor (SSTR2)-positive tissues (1–3). It has further been shown that replacing the N-terminal D-Phe in octreotide with D-Tyr allows iodination of the N-terminus and subsequent residualization of the iodinated D-amino acid (4). Therefore, in this current study we synthesized DOTA–D-Tyr<sup>1</sup>-octreotate (DOTA-DY1-TATE,

Figure 1) to allow both radiolabeling with halogens (e.g., <sup>124</sup>I, <sup>125</sup>I, <sup>131</sup>I, <sup>76</sup>Br, <sup>77</sup>Br), as well as radiometals (e.g., <sup>86</sup>Y, <sup>90</sup>Y, <sup>68</sup>Ga, <sup>177</sup>Lu, <sup>111</sup>In, <sup>64</sup>Cu). One of our goals is to achieve higher somatostatin receptor binding affinity and better target tissue uptake as well as allow halogen radionuclides to residualize in target tissues.

The use of positron-emitting halogen radionuclides, specifically <sup>124</sup>I (*t*<sub>1/2</sub> = 4.2 d) and <sup>76</sup>Br (*t*<sub>1/2</sub> = 16 h), to label radiopharmaceuticals for PET imaging has increased greatly over the past decade. For example, <sup>76</sup>Br has been labeled to octreotide (5) and <sup>76</sup>Br-labeled bromodeoxyuridine has been investigated as a tumor and brain imaging agent (6, 7). Iodine-124 is currently used to produce [<sup>124</sup>I]-5-iodo-2'-fluoro-1-β-D-arabinofuranosyl-uracil (FIAU) which has been used to image gene expression (8). Copper-64 [*t*<sub>1/2</sub> = 12.8 h; 40% β<sup>-</sup> (0.656 MeV); 19% β<sup>+</sup> (0.6 MeV); 38% EC] has diverse applications in radiopharmaceutical chemistry for PET imaging as well as therapy (9, 10). Copper-61 [*t*<sub>1/2</sub> = 3.35 h; 60% β<sup>+</sup> (1.21 MeV); 40% EC] is another cyclotron-produced positron-emitting radionuclide that is made at Washington University using the same targetry system as is used for <sup>64</sup>Cu (11). Moreover, <sup>61</sup>Cu and <sup>64</sup>Cu can be produced on demand in high yield and in high specific activity on a small biomedical cyclotron (11, 12).

The AR42J rat pancreatic carcinoma cell line is known to express SSTR2 both in vitro and in vivo (13, 14). AR42J cells grown in culture were utilized to evaluate the in vitro binding affinity and were implanted in

\* Corresponding author: Carolyn J. Anderson, Ph.D., Mallinckrodt Institute of Radiology, Washington University School of Medicine, 510 S. Kingshighway Blvd., Campus Box 8225, St. Louis, MO 63110. Phone: (314) 362-8427; fax: (314) 362-9940, e-mail: andersoncj@mir.wustl.edu.

<sup>†</sup> Washington University School of Medicine.

<sup>‡</sup> Mallinckrodt, Inc.

<sup>1</sup> Abbreviations used: DTPA, diethylenetriaminepentaacetic acid; DOTA, 1,4,7,10-tetraazacyclododecane-*N,N,N',N''*-tetraacetic acid; TETA, 1,4,8,11-tetraazacyclotetradecane-*N,N,N',N''*-tetraacetic acid; Y3, tyrosine-3; OC, octreotide; TATE, octreotate; D-Tyr<sup>1</sup>, DY1; somatostatin subtype 2 receptor, SSTR2; positron emission tomography, PET; confidence interval, CI; region of interest, ROI.

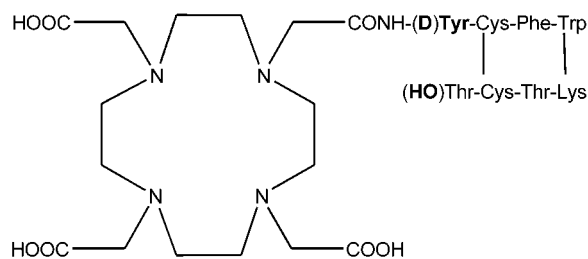


**Figure 1.** Structure of DOTA-D-Tyr<sup>1</sup>-octreotate (DOTA-DY1-TATE).

immature, normal Lewis rats for *in vivo* biodistribution and microPET imaging. In this study, we determined the *in vitro* binding affinity of copper-labeled DOTA-DY1-TATE to AR42J tumor cell membranes and investigated the *in vivo* biodistribution of <sup>64</sup>Cu-DOTA-DY1-TATE and DOTA-<sup>125</sup>I-DY1-TATE in AR42J tumor bearing rats. MicroPET imaging studies of <sup>64</sup>Cu-DOTA-DY1-TATE were carried out in the AR42J tumor-bearing SCID mice and immature Lewis rats.

## MATERIALS AND METHODS

**Materials and Analyses.** <sup>61</sup>Cu and <sup>64</sup>Cu were produced on a Cyclotron Corporation CS-15 biomedical cyclotron at Washington University of School of Medicine, using previously reported methods (11, 12). Sodium [<sup>125</sup>I]-iodide was purchased from NEN LifeScience (Boston, MA). Indium-111-chloride (<sup>111</sup>InCl<sub>3</sub>) was obtained from Mallinckrodt, Inc. (St. Louis, MO). IODO-GEN precoated iodination tubes were purchased from Pierce (Rockford, IL). Reversed-phase extraction C-18 SepPak Light cartridges were obtained from Waters (Milford, MA). Ammonium acetate (NH<sub>4</sub>OAc) was purchased from Fluka Chemical Co. (Ronkonkoma, NY); Copper acetate (99.99%) and indium acetate (99.95%) were purchased from Alfa Morton Thiokol Inc. (Danvers, MA). Trifluoroacetic acid (TFA) was obtained from J. T. Baker (Chicago, IL). All other chemicals were purchased from Aldrich Chemical Co., Inc. (Milwaukee, WI). All solutions were prepared using ultrapure water (18 MΩ-cm resistivity). Thin-layer chromatography (TLC) was performed using Whatman MKC<sub>18</sub>F reversed phase plates with 10% ammonium acetate:methanol (30:70) as the mobile phase. Radio-TLC detection was accomplished using a BIOSCAN System 200 Imaging Scanner (Washington, DC). Analytical reversed-phase HPLC was accomplished on a Waters (Milford, MA) 600E chromatography system with a Waters 991 photodiode array detector and an Ortec Model 661 (EG&G Instruments, Oak Ridge, TN) radioactive detector. Millennium 32 software (Waters, Milford, MA) was used to quantify chromatograms by integration. All HPLC samples were analyzed on a Vydac Protein & Peptide C-18 column (2.2 × 25 cm). The mobile phase was H<sub>2</sub>O (0.1% TFA) (solvent A) and 90% acetonitrile (ACN) (0.1% TFA) (solvent B). The gradient consisted of 5% B to 75% B in 25 min (1.0 mL/min flow rate). Radioactive samples were counted using a Beckman 8000 automated well-type counter (Fullerton, CA).

Preweaned (21-day old, 40–50 g) male Lewis rats were purchased from Charles River Laboratories (Boston, MA) and Female SCID-Fox Chase CB-17 mice (29–35 days old, 25–30 g) were purchased from Taconic Farms Inc (Germantown, NY). The AR42J tumor line was obtained from American Type Culture Collection (ATCC, Rockville, MD).

**Synthesis of DY1-TATE and DOTA-DY1-TATE.** The synthesis of DY1-TATE and DOTA-DY1-TATE were

accomplished by using similar methods previously described (3). Briefly, solid-phase peptide synthesis (SPPS) was carried out on an Applied Biosystems model 432A “Synergy” peptide synthesizer using the Fmoc (9-fluorenylmethoxy-carbonyl) methodology. Activated Fmoc-protected amino acids (25 μmol) were required by the instrument protocol. Activation was performed by combining 1-hydroxybenzotriazole (HOBt) and 2-(1*H*-benzotriazol-1-yl)-1,1,3,3-tetramethyluronium hexafluorophosphate (HBTU). DOTA-tris(*tert*-butyl ester) (Macrocyclics, Dallas, TX) was activated and coupled to Fmoc-protected amino acid. Final purifications of the peptides were accomplished by reversed-phase HPLC, employing a Vydac Protein & Peptide C-18 column (2.2 × 25 cm).

**Preparation of Radiolabeled Somatostatin Analogues.** DTPA-OC was labeled with <sup>111</sup>In as previously described (15). Radiolabeling with <sup>61</sup>Cu and <sup>64</sup>Cu was carried out by addition of 1–5 mCi (37–185 MBq) of <sup>61</sup>Cu or <sup>64</sup>Cu in 0.1 M ammonium acetate (pH 6.5) to 1–5 μg of the peptide in 0.1 M ammonium acetate followed by 30 min incubation at 65 °C as previously reported (16). The <sup>64/61</sup>Cu-labeled DOTA-DY1-TATE was purified on a C-18 SepPak Light cartridge, using 100% ethanol as the elution solvent, and radiochemical purity was determined by radio-TLC or radio-HPLC.

Radiiodinated DOTA-DY1-TATE was synthesized using the IODO-GEN method (17, 18). Briefly, Na [<sup>125</sup>I] [300–400 μCi (11.1–14.8 MBq)] was added to 10 μg of DOTA-DY1-TATE diluted with 0.01 M PBS (100 μL) in a glass vial coated with IODO-GEN (50 μg). The reaction mixture was removed from the reaction vessel following 25 min of incubation at room temperature. The solution was then diluted with 3 mL of water. The resulting solution was eluted through a C-18 reversed-phase extraction cartridge, which was preconditioned with 5 mL of 70% ethanol and subsequently activated with 5 mL of 2-propanol. The cartridge was rinsed successively with 5 mL of distilled water and 5 mL of 0.5 M acetic acid. The radiiodinated peptide was eluted in 5 mL of 96% ethanol, and the solvent was evaporated at room temperature under a gentle stream of nitrogen. The dry residue was reconstituted in 1–3 mL of 0.9% NaCl.

The cold copper and indium agents (<sup>nat</sup>Cu-DOTA-DY1-TATE, <sup>nat</sup>Cu-DOTA-Y3-TATE, <sup>nat</sup>In-DTPA-OC) for the receptor binding assays were prepared by the reaction of copper and indium acetate using the same procedure described above for radiolabeling of DOTA-DY1-TATE with <sup>61</sup>Cu, <sup>64</sup>Cu, and <sup>111</sup>In. DOTA-<sup>nat</sup>I-DY1-TATE was synthesized by following the same procedure as for DOTA-<sup>125</sup>I-DY1-TATE, and the reaction yield was confirmed by HPLC.

**In Vitro Receptor Binding Assay.** The binding affinity of Cu-DOTA-DY1-TATE was measured in AR42J rat pancreatic tumor membranes using methods previously described with minor modifications (9). Briefly, <sup>61</sup>Cu-DOTA-DY1-TATE was displaced with increasing concentrations of <sup>nat</sup>Cu-DOTA-DY1-TATE. A competitive binding assay was performed by displacing <sup>111</sup>In-DTPA-OC with the competing ligands <sup>nat</sup>Cu-DOTA-DY1-TATE, <sup>nat</sup>Cu-DOTA-Y3-TATE, <sup>nat</sup>In-DTPA-OC and DOTA-<sup>nat</sup>I-DY1-TATE. Assays were carried out using the Millipore Multiscreen system (Bedford, MA) (9). The best-fit IC<sub>50</sub> values, the dissociation constant (*K<sub>d</sub>*), and the number of SSTR2 binding sites (*B<sub>max</sub>*) for the AR42J cells were calculated using PRISM (Graphpad, San Diego, CA).

**Animal Models.** All animal experiments were performed in compliance with the Guidelines for the Care and Use of Research Animals established by Washington

University's Animal Studies Committee. For AR42J tumor-bearing mice, AR42J cells were grown as xenografts in female SCID mice. Briefly, AR42J cells ( $1 \times 10^7$ ), grown in F-12K Nutrient mixture medium containing 20% fetal calf serum (FCS) were injected subcutaneously, bilaterally, into flanks and necks of female SCID mice (19). The tumors were allowed to grow 10–12 days until 0.5–0.9 g in size. Male Lewis rats (21 d old) were implanted with AR42J tumors in the necks or/and left legs from tumor obtained from Mallinckrodt, Inc (St. Louis, MO) (passage 36) and maintained by serial passage in animals. Tumor was excised from euthanized rats and was rinsed with sterile saline and placed on ice in a Petri dish containing Gibco Media 199 (Sigma Chemical Co., St. Louis, MO). Connective and necrotic tissue were removed, and the material was diced into small pieces ( $2 \times 2$  mm). The freshly dissected pieces were delivered to the left flank of the animal via a 13-gauge trocar inserted subcutaneously. AR42J tumor growth was observed for 2 weeks after implantation, and tumors achieved a solid, palpable mass of 1.0–1.5 g in size by ~14 days postimplantation.

**Biodistribution of  $^{64}\text{Cu}$ -DOTA-DY1-TATE and DOTA- $^{125}\text{I}$ -DY1-TATE.** Biodistribution studies were carried out using immature (~33 day old) male Lewis rats bearing AR42J tumors (12 days post-implant) in the left flank. Anesthetized animals received a coinjection of  $^{64}\text{Cu}$ -DOTA-DY1-TATE and DOTA- $^{125}\text{I}$ -DY1-TATE (32  $\mu\text{Ci}$  for  $^{64}\text{Cu}$ , 5  $\mu\text{Ci}$  for  $^{125}\text{I}$ , 0.68  $\mu\text{g}$  peptide for each compound) via the tail vein. The animals were euthanized at 1, 4, 24, and 72 h postinjection. A group of 5 rats were coinjected with a blocking dose of DY1-TATE (150  $\mu\text{g}$ ) and sacrificed 1 h postinjection. Following euthanization, the tissues and organs of interest were removed and weighed, and the radioactivity was measured in a gamma counter. Standards ( $n = 5$ ) were prepared to verify the counting efficiency of the gamma counter for each radionuclide. Samples were first counted for  $^{64}\text{Cu}$  using a specific energy window that did not have detectable crossover for  $^{125}\text{I}$ . After allowing for complete decay of the  $^{64}\text{Cu}$  ( $>12$  half-lives), the samples were then counted using the energy window specific for  $^{125}\text{I}$ . The percent injected dose per gram (% ID/g) and percent injected dose per organ (% ID/organ) were calculated by comparison with standards representing the injected dose per animal. A group of five rats that were sacrificed at 72 h postinjection were housed in individual metabolism cages for the collection of urine and feces at various time points from 1 to 72 h for determination of the %ID excreted.

**MicroPET Images.** Positron emission tomography (PET) imaging was performed on the first commercially available microPET (Concorde Microsystems, Knoxville, TN) which was based on the design of Cherry and colleagues (20). Imaging studies were carried out on four SCID mice and four male Lewis rats carrying AR42J tumors. Two mice bearing tumors on the neck and left leg and four rats (two rats had tumors on neck and left leg, the other two rats had tumors on left legs only) were imaged on the microPET at selected times postinjection. Two tumor-bearing mice were each injected with 1 mCi  $^{64}\text{Cu}$ -DOTA-DY1-TATE (1 mCi/ $\mu\text{g}$  for control, 1 mCi/50  $\mu\text{g}$  for blocked) and imaged at 10 min, 1, 2, and 4 h postinjection. The two mice were imaged side by side and remained in the same bed position for all time points. Four rats were each injected with 2.5 mCi  $^{64}\text{Cu}$ -DOTA-DY1-TATE (2.5 mCi/ $\mu\text{g}$  for control, 2.5 mCi/150  $\mu\text{g}$  for blocked) and imaged at 10 min, 1, 2, and 4 h. Each rat was imaged in two bed positions. Immediately after

imaging, the %ID/g of tumor from the rats was determined by measuring the dissected tumors in a dose calibrator (Capintec, Ramsey, NJ). Tumor, kidney, and liver activities of  $^{64}\text{Cu}$  were generated by measuring regions of interest (ROIs) that encompassed the entire organ from the microPET images in AR42J tumor-bearing SCID mice and Lewis rats after 2 and 4 h postinjection.

**Statistical Methods.** To compare differences between the data, a student's t-test was performed using Prism (Graphpad, San Diego, CA). Differences at the 95% confidence level ( $p < 0.05$ ) were considered significant.

## RESULTS

**Chemistry and Radiochemistry.** The DY1-TATE and DOTA-DY1-TATE were analyzed by analytical reversed-phase HPLC (UV detection 214 nm) using conditions described in the Methods section and by LC-MS. DY1-TATE: HPLC retention time = 17.9 min; MS,  $m/z$  calculated for  $\text{C}_{49}\text{H}_{64}\text{N}_{10}\text{O}_{12}\text{S}_2$  ( $\text{M} + \text{H}$ ) $^+$  = 1048.4, found 1049.3. DOTA-DY1-TATE: HPLC retention time = 20.4 min; MS,  $m/z$  calculated for  $\text{C}_{65}\text{H}_{90}\text{N}_{14}\text{O}_{19}\text{S}_2$  ( $\text{M} + \text{H}$ ) $^+$  = 1434.7, found 1435.6.  $^{111}\text{In}$ -DTPA-OC and  $^{61/64}\text{Cu}$ -DOTA-DY1-TATE were prepared in  $\geq 98\%$  radiochemical purity. Specific activities for both  $^{111}\text{In}$ - and  $^{61/64}\text{Cu}$ -labeled conjugates ranged from 1500 to 3500 Ci/mmol (56000 to 111000 GBq/mmol). The radiochemical purity of DOTA- $^{125}\text{I}$ -DY1-TATE was confirmed to be greater than 98% by radio-HPLC. DOTA-DY1-TATE was typically labeled with  $^{125}\text{I}$  to a specific activity of 300 Ci/mmol (11000 GBq/mmol). The reaction yields for "cold" somatostatin analogues were greater than 98% as confirmed by radio-TLC of an exchange reaction between natural  $\text{Cu}^{2+}$  or  $\text{In}^{3+}$  with  $^{64}\text{Cu}$  or  $^{111}\text{In}$ , respectively.

**In Vitro Receptor Binding Assay.** A homogeneous competitive binding assay was performed using AR42J tumor membranes, where  $^{61}\text{Cu}$ -DOTA-DY1-TATE was challenged with increasing concentrations of  $^{nat}\text{Cu}$ -DOTA-DY1-TATE. The  $\text{IC}_{50}$  value for  $^{nat}\text{Cu}$ -DOTA-DY1-TATE was determined to be 1.35 nM, with a 95% confidence interval (CI) of 1.02 to 1.8 nM (Figure 2A). Scatchard analysis of the data showed a  $K_d$  of 176.4 pM (95% CI 158.4 to 201.3 pM) and a somatostatin  $B_{\text{max}}$  in the AR42J membranes of 244.4 fmol/mg (95% CI 219.7 to 274.1 fmol/mg) of membrane protein (Figure 2B).

A competitive binding assay was performed between four somatostatin analogues vs  $^{111}\text{In}$ -DTPA-OC. The concentration of the radioligand in the binding assays was 0.05 nM. The  $\text{IC}_{50}$  values were 1.78 nM for Cu-DOTA-Y3-TATE, 4.62 nM for Cu-DOTA-DY1-TATE, 4.8 nM for DOTA-I-DY1-TATE, and 4.87 nM for In-DTPA-OC (Figure 3 and Table 1). These results suggest that Cu-DOTA-DY1-TATE and DOTA-I-DY1-TATE have similar binding affinity to AR42J cells as In-DTPA-OC, while the analogue with Tyr in the 3-position has somewhat higher binding affinity.

**Biodistribution Studies.** Summaries of the biodistribution data are shown in Figure 4. Rapid clearance of the radioactivity from the blood circulation was observed for both compounds. At all times of analysis the average uptake of  $^{64}\text{Cu}$  activity in tumors was approximately twice as high as  $^{125}\text{I}$  activity ( $p < 0.03$ ). The highest tumor uptake of  $^{64}\text{Cu}$ -DOTA-DY1-TATE ( $1.515 \pm 0.154$  %ID/g) was found after 1 h postinjection, and was  $1.247 \pm 0.250$  %ID/g at 4 h postinjection, suggesting that the  $^{64}\text{Cu}$  was residualized in the tumor out to at least 4 h postinjection. A similar trend was observed for DOTA- $^{125}\text{I}$ -DY1-TATE ( $0.814 \pm 0.058$  %ID/g at 1 h,  $0.543 \pm 0.016$

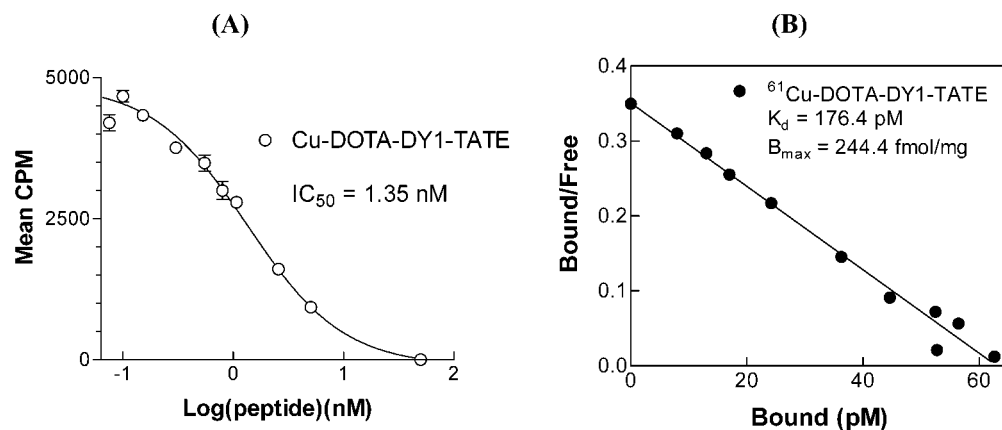


**Figure 2.** The in vitro binding affinity of  $^{61}\text{Cu}$ -DOTA-DY1-TATE to AR42J rat pancreatic tumor membranes blocked with increasing concentrations of unlabeled Cu-DOTA-DY1-TATE ( $n = 6$  for each data point).

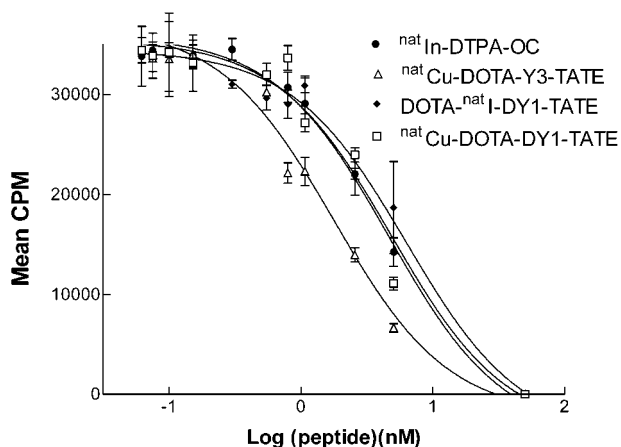


**Figure 3.** Competitive binding assay of Cu-DOTA-DY1-TATE, DOTA-I-DY1-TATE, Cu-DOTA-Y3-TATE, and In-DTPA-OC displacing  $^{111}\text{In}$ -DTPA-OC in AR42J tumor membranes ( $n = 3$  for each data point).

**Table 1.  $\text{IC}_{50}$  Values for Competitive Binding Assay of  $^{\text{nat}}\text{Cu}$ -DOTA-DY1-TATE,  $\text{DOTA}^{\text{nat}}\text{I}$ -DY1-TATE,  $^{\text{nat}}\text{Cu}$ -DOTA-Y3-TATE, and  $^{\text{nat}}\text{In}$ -DTPA-OC Displacing  $^{111}\text{In}$ -DTPA-OC in AR42J Tumor Membranes ( $n = 3$  for each data point)**

competing ligand	$\text{IC}_{50}$ (nM)	95% CI (nM)
$^{\text{nat}}\text{Cu}$ -DOTA-Y3-TATE	1.78	1.29–2.46
$^{\text{nat}}\text{Cu}$ -DOTA-DY1-TATE	4.62	3.28–6.52
$\text{DOTA}^{\text{nat}}\text{I}$ -DY1-TATE	4.58	3.13–6.69
$^{\text{nat}}\text{In}$ -DTPA-OC	4.87	3.98–5.96

%ID/g at 4 h) in the tumors. In the rats that received the co-injected blocking dose, the uptake in the tumor of  $^{64}\text{Cu}$ -DOTA-DY1-TATE ( $0.468 \pm 0.046$  %ID/g) and  $\text{DOTA}^{125}\text{I}$ -DY1-TATE ( $0.323 \pm 0.016$  %ID/g) was significantly lower at 1 h postinjection ( $p < 0.02$ ) (Table 2). The higher uptake of  $^{64}\text{Cu}$ -labeled conjugate in the tumor compared to  $^{125}\text{I}$ -labeled conjugate may be due to a greater degree of retention of  $^{64}\text{Cu}$ -DOTA-DY1-TATE in the tumor compared to  $\text{DOTA}^{125}\text{I}$ -DY1-TATE. Since time points earlier than 1 h were not evaluated for the biodistribution studies, it is difficult to know whether the uptake of  $\text{DOTA}^{125}\text{I}$ -DY1-TATE in the tumor peaked prior to 1 h.

The uptake in the pituitary and the pancreas at 1 h postinjection was significantly higher with  $^{64}\text{Cu}$ -DOTA-DY1-TATE ( $1.985 \pm 0.334$  %ID/g for pituitary,  $1.490 \pm 0.337$  %ID/g for pancreas) compared with  $\text{DOTA}^{125}\text{I}$ -DY1-TATE ( $1.246 \pm 0.160$  %ID/g for pituitary,  $0.850 \pm 0.203$  %ID/g for pancreas) ( $p < 0.05$ ). Uptake in the SSTR2-rich pituitary, adrenals, and pancreas was blocked

with unlabeled DY1-TATE for both the  $^{125}\text{I}$  and  $^{64}\text{Cu}$ -labeled peptides, suggesting receptor-mediated uptake of both compounds in these tissues (Table 2). No appreciable differences were observed for non-somatostatin-receptor-positive tissues between rats that received a coinjection of blocking dose and unblocked rats.

Liver uptake for  $\text{DOTA}^{125}\text{I}$ -DY1-TATE at all times of analysis was lower than for  $^{64}\text{Cu}$ -DOTA-DY1-TATE. However, the kidney uptake of  $\text{DOTA}^{125}\text{I}$ -DY1-TATE ( $9.761 \pm 1.036$  %ID/g at 1 h,  $9.450 \pm 0.255$  %ID/g at 4 h,  $8.190 \pm 0.646$  %ID/g at 24 h,  $5.921 \pm 0.880$  %ID/g at 72 h) was 3-fold higher than that of  $^{64}\text{Cu}$ -DOTA-DY1-TATE ( $2.888 \pm 0.187$  %ID/g at 1 h,  $2.389 \pm 0.202$  %ID/g at 4 h,  $1.740 \pm 0.061$  %ID/g at 24 h,  $1.206 \pm 0.158$  %ID/g at 72 h). The kidney clearance of  $\text{DOTA}^{125}\text{I}$ -DY1-TATE maintained a level of  $5.921 \pm 0.880$  %ID/g even after 72 h postinjection. This high kidney uptake and longer retention time of  $\text{DOTA}^{125}\text{I}$ -DY1-TATE was similar to that of  $^{125}\text{I}$ -DY1-TATE and  $\text{DTPA}^{125}\text{I}$ -DY1-TATE (4). This is most likely due to the longer residence time of the  $\text{DOTA}^{125}\text{I}$ -DY1 residue in the kidneys compared to  $^{125}\text{I}$ -L-amino acids. Except for  $^{125}\text{I}$  activity in thyroid, normal tissue uptake of  $\text{DOTA}^{125}\text{I}$ -DY1-TATE decreased throughout the period.

The highest tumor: blood ratios were found at 4 h postinjection for both  $^{64}\text{Cu}$ - and  $^{125}\text{I}$ -labeled DOTA-DY1-TATE in AR42J tumor-bearing Lewis rats ( $7.8 \pm 1.5$  and  $8.8 \pm 0.9$ , respectively). For  $\text{DOTA}^{125}\text{I}$ -DY1-TATE, the tumor-to-blood ratio maintained at high levels out to 24 h postinjection ( $6.4 \pm 1.0$ ), while for  $^{64}\text{Cu}$ -DOTA-DY1-TATE the ratio dropped to  $2.6 \pm 0.6$ . Tumor:muscle ratios were similar for  $^{64}\text{Cu}$ - and  $^{125}\text{I}$ -labeled DOTA-DY1-TATE, with the peak ratio occurring at 4 h ( $19.2 \pm 3.8$  and  $21.9 \pm 2.5$ , respectively).

The excretion data demonstrated that  $59.18 \pm 21.05$  %ID for  $^{64}\text{Cu}$  and  $64.22 \pm 19.93$  %ID for  $^{125}\text{I}$  was excreted from the urine by 4 h postinjection. By 24 h postinjection,  $\sim 75$  %ID of  $^{64}\text{Cu}$ -DOTA-DY1-TATE activity was found in the urine and feces, and  $\sim 85$  %ID of  $\text{DOTA}^{125}\text{I}$ -DY1-TATE activity was excreted (Table 3).

**MicroPET Images.** Figure 5A shows the coronal microPET images of AR42J tumor-bearing SCID mice, 2 h postadministration of  $^{64}\text{Cu}$ -DOTA-DY1-TATE, with and without a coinjected blocking dose of DY1-TATE. Uptake in the neck and thigh tumors was visible at 2 h postinjection for the control mouse (left). Conversely, the other mouse (right) that received a blocking dose showed reduced uptake at both tumor sites. Prominent uptake was observed in the liver and kidneys in both animals.

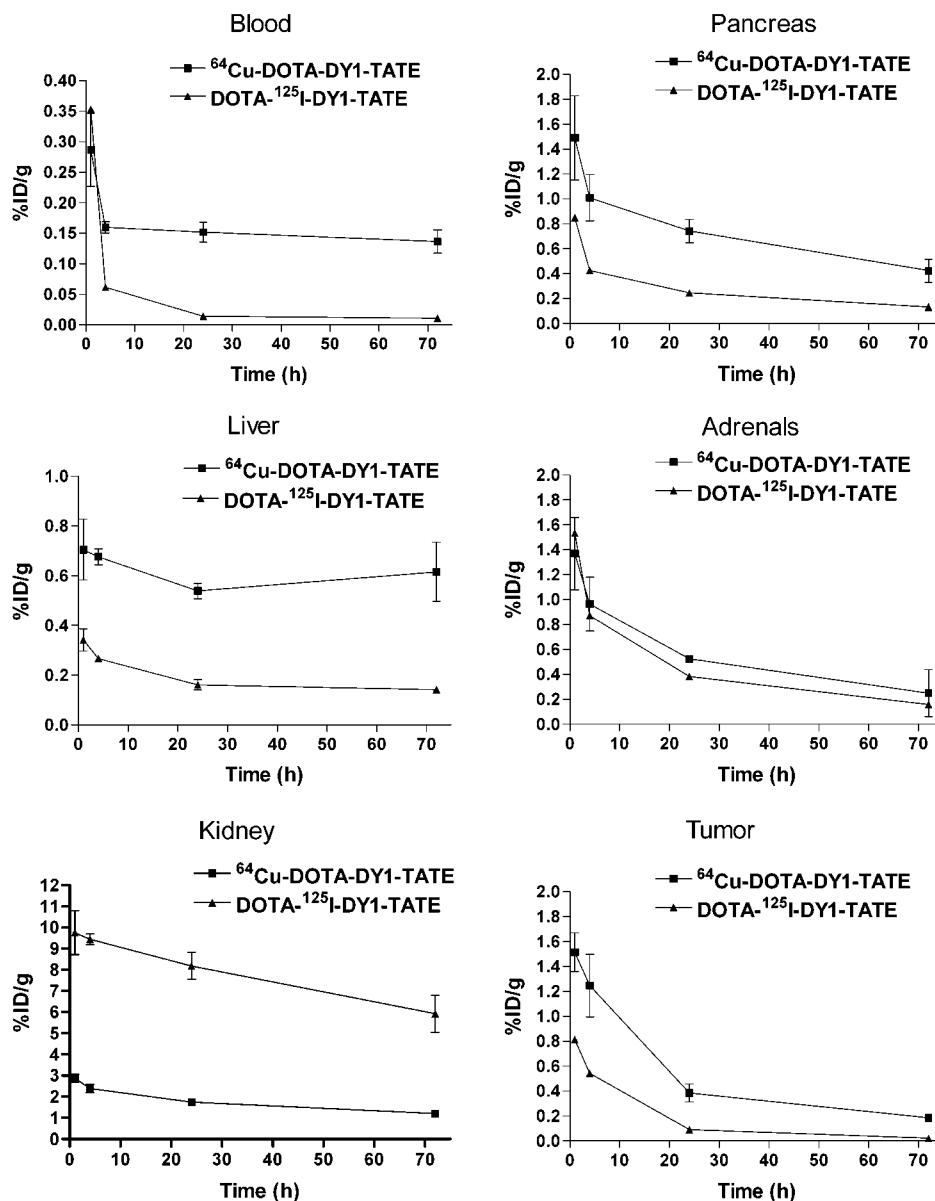


**Figure 4.** Biodistribution data of  $^{64}\text{Cu}$ -DOTA-DY1-TATE and DOTA- $^{125}\text{I}$ -DY1-TATE in normal and SSTR2 positive tissues (blood, liver and kidneys, pancreas, adrenals, tumor). Data are presented as %ID/g  $\pm$  SD,  $n = 5$  for each time point.

**Table 2.** Biodistribution of  $^{64}\text{Cu}$ -DOTA-DY1-TATE and DOTA- $^{125}\text{I}$ -DY1-TATE in AR42J Tumor Bearing Lewis Rats at 1 h, with and without a Coadministration of Blocking Agent<sup>a</sup>

tissue	$^{64}\text{Cu}$ , 1 h	$^{64}\text{Cu}$ , 1 h block	$^{125}\text{I}$ , 1 h	$^{125}\text{I}$ , 1 h block
blood	0.287 $\pm$ 0.060	0.361 $\pm$ 0.065	0.354 $\pm$ 0.073	0.434 $\pm$ 0.064
liver	0.705 $\pm$ 0.122	0.981 $\pm$ 0.199	0.342 $\pm$ 0.045	0.352 $\pm$ 0.036
kidney	2.888 $\pm$ 0.187	3.626 $\pm$ 0.176	9.761 $\pm$ 1.036	10.895 $\pm$ 0.863
pituitary	1.985 $\pm$ 0.334	0.516 $\pm$ 0.456	1.246 $\pm$ 0.160	0.325 $\pm$ 0.208
adrenals	1.369 $\pm$ 0.291	0.234 $\pm$ 0.066	1.534 $\pm$ 0.351	0.212 $\pm$ 0.036
pancreas	1.490 $\pm$ 0.337	0.409 $\pm$ 0.059	0.850 $\pm$ 0.203	0.270 $\pm$ 0.024
tumor	1.515 $\pm$ 0.154	0.468 $\pm$ 0.046	0.814 $\pm$ 0.058	0.323 $\pm$ 0.016
thyroid	0.307 $\pm$ 0.040	0.388 $\pm$ 0.083	1.357 $\pm$ 0.131	1.234 $\pm$ 0.023

<sup>a</sup> Data are presented as % ID/g  $\pm$  SD ( $n = 5$ ).

Four hours after administration of  $^{64}\text{Cu}$ -DOTA-DY1-TATE, both tumor sites in the nonblocked animal could still be easily identified, as well as showing higher uptake than other normal organs.

Figure 5B shows the microPET images in Lewis rats bearing AR42J tumors of  $^{64}\text{Cu}$ -DOTA-DY1-TATE obtained after 2 h postinjection with and without the addition of DY1-TATE as a blocking agent. Imaging was performed at 1, 2, and 4 h postinjection. Similar to the

AR42J tumor-bearing mice images, tumor uptake was also observed in the tumor-bearing rats. The most prominent region of  $^{64}\text{Cu}$ -DOTA-DY1-TATE uptake was the bladder, due to the rapid excretion of this compound into the urine. In addition, significant uptake in the SSTR2-rich pituitary was observed.

Uptake of radioactivity in the tumor, kidney, and liver measured from the microPET images in the AR42J tumor-bearing SCID mice and Lewis rats after 2 and 4

**Table 3. Excretion of  $^{64}\text{Cu}$ -DOTA-DY1-TATE and DOTA- $^{125}\text{I}$ -DY1-TATE in AR42J Tumor-Bearing Lewis Rats<sup>a</sup>**

	$^{64}\text{Cu}$ -DOTA-DY1-TATE			DOTA- $^{125}\text{I}$ -DY1-TATE		
	4 h	24 h	48 h	4 h	24 h	48 h
urine	59.18 ± 21.05	65.36 ± 19.88	66.29 ± 20.35	64.22 ± 19.93	74.93 ± 21.77	77.76 ± 20.34
feces	<0.1	9.08 ± 9.45	11.12 ± 9.87	<0.1	9.79 ± 8.97	12.39 ± 5.42

<sup>a</sup> All data are reported as % ID ± SD ( $n = 5$ ).

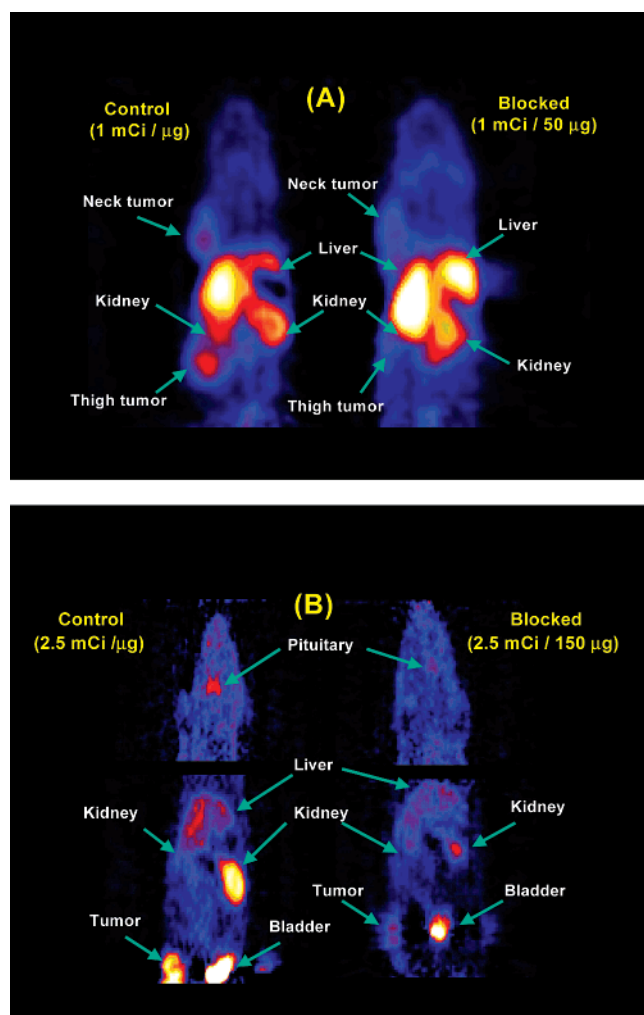


**Figure 5.** (A) Coronal microPET images of AR42J tumor-bearing SCID mice after 2 h postadministration of  $^{64}\text{Cu}$ -DOTA-DY1-TATE, with and without a coinjected blocking dose (2.5 mCi/ $\mu\text{g}$ , left; 2.5 mCi/ $\mu\text{g}$  coinjected with 50  $\mu\text{g}$  of DY1-TATE, right). (B) Coronal microPET images of AR42J tumor-bearing Lewis rats (2 bed positions) after 2 h postadministration of  $^{64}\text{Cu}$ -DOTA-DY1-TATE, with and without a coinjected blocking dose (2.5 mCi/ $\mu\text{g}$ , left; 2.5 mCi/ $\mu\text{g}$  coinjected with 150  $\mu\text{g}$  of DY1-TATE, right).

h postinjection are given in Figures 6A and 6B. In the SCID mice, the results suggested tumor activity in the control mice (0.02  $\mu\text{Ci}/\mu\text{L}$  at 2 h pi, 0.02  $\mu\text{Ci}/\mu\text{L}$  at 4 h pi) was about 2-fold higher than in blocked mice (0.01  $\mu\text{Ci}/\mu\text{L}$  for 2 h pi, 0.01  $\mu\text{Ci}/\mu\text{L}$  for 4 h pi). In SCID mice, the tumor activity was similar at both 2 and 4 h postinjection. In the 'blocked' Lewis rats, a similar reduction in activity was observed compared to control Lewis rats. Tumor activity in the control rats (0.03  $\mu\text{Ci}/\mu\text{L}$  for 2 h pi, 0.02  $\mu\text{Ci}/\mu\text{L}$  for 4 h pi) was 2–3-fold higher than in 'blocked' rats (0.01  $\mu\text{Ci}/\mu\text{L}$  for 2 h pi, 0.01  $\mu\text{Ci}/\mu\text{L}$  for 4 h pi). These results agreed with tumor uptake measurements that were determined by measuring the activity of the dissected tumor in a dose calibrator, where  $4.14 \pm 0.01$  %ID/g was found in the control tumor and  $1.46 \pm 0.00$

%ID/g was in the tumor of the rat coinjected with blocking agent. These data confirmed that tumor uptake was blocked with an excess of DY1-TATE. Moreover, blocking of tumor activity in the rats appeared to be more effective than in mice, which probably reflects the crossover activity from liver/kidney in mice that obscures the tumor, especially in the blocked mice when measuring regions of interest (ROIs) that encompassed the entire organ.

## DISCUSSION

The utility of radiolabeled somatostatin analogues for imaging and therapy of cancer is well described in the literature. The majority of newly developed somatostatin analogues were specifically designed for labeling radiometals (1–3). The goal of this research was to design a somatostatin analogue for labeling both radiometals and halogens, with the added feature of having the halogen residualized in target tissue. Here we investigated DOTA-DY1-TATE, where the C-terminal alcohol of octreotide was replaced with a C-terminal acid (TATE). This analogue was labeled with  $^{64}\text{Cu}$  and  $^{125}\text{I}$  and compared in in vitro receptor binding assays and in vivo somatostatin-receptor-positive tumor-bearing animal models. Having a somatostatin analogue that allows the ability for labeling both metals and halogens will allow direct comparisons of these analogues with the only modification being the radionuclide used for labeling.

Receptor binding experiments using AR42J rat pancreatic tumor membranes were performed to verify the  $\text{IC}_{50}$  values of the new somatostatin analogues compared to  $^{111}\text{In}$ -DTPA-OC. Scatchard analysis was performed with  $^{61}\text{natCu}$ -DOTA-DY1-TATE to determine the  $K_d$  of this analogue. The unlabeled iodinated and copper complexed DOTA-DY1-TATE analogues had binding affinity that were comparable to In-DTPA-OC while the  $\text{IC}_{50}$  for Cu-DOTA-Y3-TATE was about 2–3-fold lower. These data are encouraging, since it demonstrates that the binding affinity was not compromised with the DY1-TATE analogues compared to the DTPA-OC and DOTA-Y3-TATE analogues. Another DY1 analogue (DTPA- $^{125}\text{I}$ -DY1-OC) was described by Breeman et al. (4); however, this analogue had an  $\text{IC}_{50}$  value vs  $^{125}\text{I}$ -Y3-OC that was 200-fold higher than  $^{125}\text{I}$ -Y3-OC itself.

The biodistribution of  $^{64}\text{Cu}$ - and  $^{125}\text{I}$ -labeled DOTA-DY1-TATE were performed in one coinjection experiment in AR42J tumor-bearing Lewis rats. This model has several advantages compared to the typically utilized animal models, AR42J tumor-bearing nude/SCID mice, and CA20948-tumor bearing rats. AR42J cells grow both in cell culture and in animal models, which allows the advantage of comparing in vitro receptor binding studies and tumor-bearing animal studies using the same tumor cell line. The use of young rats (21 d) also allows the AR42J tumor cells to be implanted into immunocompetent rodents, rather than immunocompromised nude or SCID mice.

Greater somatostatin-receptor-mediated uptake was observed with  $^{64}\text{Cu}$ -DOTA-DY1-TATE than DOTA- $^{125}\text{I}$ -DY1-TATE in the pancreas as well as the AR42J tumor ( $p < 0.02$ ), whereas the uptake was similar in the

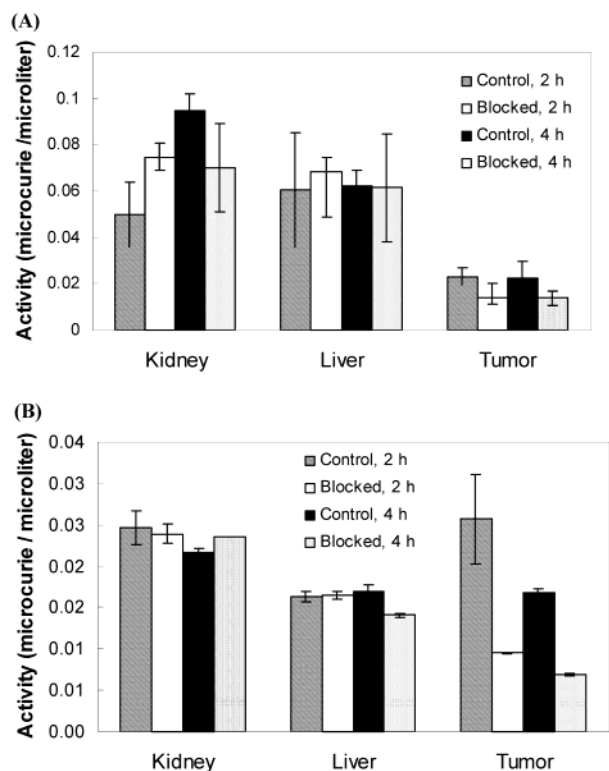


**Figure 6.** Tumor, kidney, and liver activity of  $^{64}\text{Cu}$  after 2 and 4 h postadministration of  $^{64}\text{Cu}$ -DOTA-DY1-TATE generated by measuring ROIs from microPET images in control and blocked AR42J tumor-bearing SCID mice (A) and Lewis rats (B). Each bar presents two animals.

adrenals. However, the liver and blood uptake of  $^{64}\text{Cu}$ -DOTA-DY1-TATE were significantly greater than for DOTA- $^{125}\text{I}$ -DY1-TATE ( $p < 0.01$ ). The high uptake in the blood at longer time points and the increasingly high uptake in the liver was problematic for  $^{64}\text{Cu}$ -DOTA-DY1-TATE, suggesting that  $^{64}\text{Cu}$  dissociated from the DOTA chelator (21). Research is ongoing to develop more stable chelators for copper radionuclides that have greater kinetic stability, and these will eventually be conjugated to somatostatin analogues (22). It is predicted that conjugating a chelator to DY1-TATE that forms a more stable Cu(II) complex than DOTA will significantly decrease accumulation in the blood, liver and kidneys.

The uptake of  $^{64}\text{Cu}$ - and  $^{125}\text{I}$ -labeled DOTA-DY1-TATE was not as high in somatostatin-receptor positive tissues as has been observed for other radiolabeled somatostatin analogues. Comparisons between the AR42J tumor-bearing rat model can only be made with CA20948 tumor-bearing rats, since to the best of our knowledge, uptake of radiolabeled somatostatin analogues has not yet been reported for the AR42J tumor-bearing rat model. Therefore, comparisons with other somatostatin-receptor positive tissues are presented here. For example, the uptake of  $^{64}\text{Cu}$ -TETA-Y3-TATE in the rat pancreas was  $9.35 \pm 1.66$  %ID/g in Lewis rats (19) at 1 h postinjection, compared to  $1.49 \pm 0.34$  %ID/g for  $^{64}\text{Cu}$ -DOTA-DY1-TATE and  $0.85 \pm 0.20$  %ID/g for DOTA- $^{125}\text{I}$ -DY1-TATE. A biodistribution study of  $^{177}\text{Lu}$ -DOTA-Y3-TATE in Lewis rats showed a pancreas uptake of  $10.49 \pm 1.91$  %ID/g (23). However, the uptake of the DOTA-DY1-TATE analogues in the pancreas was comparable or greater than  $^{64}\text{Cu}$ -TETA-OC ( $0.86 \pm 0.14$  %ID/g) and  $^{111}\text{In}$ -DTPA-OC ( $0.42 \pm 0.09$  %ID/g) (15). Compared to DTPA- $^{125}\text{I}$ -DY1-OC (4), the pancreas and adrenal uptakes of DOTA- $^{125}\text{I}$ -DY1-TATE were somewhat higher (pan-

creas:  $0.85$  vs  $\sim 0.5$  %ID/g, respectively; adrenal:  $1.5$  vs  $\sim 1.0$  %ID/g, respectively). This suggests that the octreotate analogues may be superior to the octreotide analogues, which has been previously been reported (2, 3).

Although the radiometal-labeled DOTA/TETA-Y3-TATE analogues showed superior receptor-mediated uptake, these analogues do not allow the ability to label via a residualizing label with radiohalogens. Therefore, the use of the DY1 analogues opens possibilities for the radiotherapeutic application of radiohalogenated ligands in patients with somatostatin receptor-positive tumors.

MicroPET imaging of  $^{64}\text{Cu}$ -DOTA-DY1-TATE in AR42J tumor-bearing mice and rats at 2 h postinjection showed higher amounts of activity in the liver and kidneys compared to other normal tissues (Figure 6). The tumor also had significant uptake and showed good contrast compared with receptor-negative background tissue in the neck and thigh tumors of the mouse, and the thigh tumors in the rat model. In the AR42J-tumor bearing Lewis rats, the somatostatin receptor-positive pituitary was visualized, whereas it was not visualized in the rat co-injected with a blocking dose. Quantification of the activity in the rat tumor, liver, and kidney was comparable to the relative amounts determined by traditional biodistribution. The quantification of the microPET images also demonstrated that the activity in the tumor was significantly blocked, and this decrease in uptake corresponded to the visual decrease in uptake delineated in the images. These data suggest that microPET may be used as an alternative to traditional multiple animal biodistribution studies for screening new positron-emitting radiopharmaceuticals.

## CONCLUSIONS

The study presented here demonstrates that DOTA-DY1-TATE is a peptide that can be labeled with both metal and halogen radionuclides. The  $\text{IC}_{50}$  values for  $^{64}\text{Cu}$ - and  $^{125}\text{I}$ -labeled DOTA-DY1-TATE were comparable to  $^{111}\text{In}$ -DTPA-OC, and these analogues showed somatostatin receptor-mediated uptake in normal and tumor tissues in vivo. DOTA- $^{125}\text{I}$ -DY1-TATE appeared to remain in the tumor out to 4 h postinjection, suggesting that the iodine was possibly residualized in the tumor cells. Future studies include microPET imaging in the AR42J tumor-bearing rat model with DOTA-DY1-TATE labeled with other positron-emitting radionuclides such as  $^{76}\text{Br}$ ,  $^{124}\text{I}$ , and  $^{86}\text{Y}$ .

## ACKNOWLEDGMENT

The authors wish to thank Lynne Jones, Nicole Mercer, Mu Wang, Virginia Richey, and John Engelbach for technical assistance, and W. Barry Edwards, Ph.D. (MetaPhore Pharmaceuticals) for helpful discussions. This research was supported by NIH Grant R01 CA64475 (C.J.A.). The production of copper radionuclides at Washington University is supported by a grant from the National Cancer Institute (R24 CA86307 – M. J. Welch, P. I.). MicroPET imaging is supported by NIH/NCI SAIRP grant (1R24 CA83060). We would also like to thank the Small Animal Imaging Core of the Alvin J. Siteman Cancer Center at Washington University and Barnes Jewish Hospital in St. Louis, MO for additional support of the microPET imaging. The core is supported by a NCI Cancer Center Support Grant (1P30 CA91842).

## LITERATURE CITED

- de Jong, M., Bakker, W. H., Breeman, W. A. P., Bernard, B. F., Hofland, L. J., Visser, T. J., Srinivasan, A., Schmidt, M., Behe, M., Maecke, H., and Krenning, E. P. (1998) Pre-

- Clinical Comparison of [DTPA<sup>0</sup>]Octreotide, [DTPA<sup>0</sup>Tyr<sup>3</sup>]-Octreotide and [DOTA<sup>0</sup>Tyr<sup>3</sup>]Octreotide as Carriers for Somatostatin Receptor-Targeted Scintigraphy and Radionuclide Therapy. *Int. J. Cancer* 75, 406–411.
- (2) de Jong, M., Breeman, W. A. P., Bakker, W. H., Kooij, P. P. M., Bernard, B. F., Hofland, L. J., Visser, T. J., Srinivasan, A., Schmidt, M., Erion, J. L., Bugaj, J. E., Maেকে, H. R., and Krenning, E. P. (1998) Comparison of <sup>111</sup>In-Labeled Somatostatin Analogues for Tumor Scintigraphy and Radionuclide Therapy. *Cancer Res.* 58, 437–441.
  - (3) Lewis, J. S., Lewis, M. R., Srinivasan, A., Schmidt, M. A., Wang, J., and Anderson, C. J. (1999) Comparison of Four <sup>64</sup>Cu-labeled Somatostatin Analogues in vitro and in a Tumor-bearing Rat Model: Evaluation of New Derivatives for PET Imaging and Targeted Radiotherapy. *J. Med. Chem.* 42, 1341–1347.
  - (4) Breeman, W. A. P., de Jong, M., Bernard, B., Hofland, L. J., Srinivasan, A., Vanderpluijm, M., Bakker, W. H., Visser, T. J., and Krenning, E. P. (1998) Tissue Distribution and Metabolism of Radioiodinated DTPA(0), D-Tyr(1) and Tyr(3) Derivatives of Octreotide in Rats. *Anticancer Res.* 18(1A), 83–89.
  - (5) Yngve, U., Khan, T. S., Bergstrom, M., and Langstrom, B. (2001) Labeling of Octreotide using Br-76-prosthetic Groups. *J. Lab. Compd. Radiopharm.* 44, 561–573.
  - (6) Gardelle, O., Roelcke, U., Vontobel, P., Crompton, N. E. A., Guenther, I., Blauenstein, P., Schubiger, P. A., Blattmann, H., Ryser, J. E., Leenders, K. L., and Kaser-Hotz, B. (2001) [Br-76]bromodeoxyuridine PET in Tumor-bearing Animals. *Nucl. Med. Biol.* 28, 51–57.
  - (7) Ryser, J. E., Blauenstein, P., Remy, N., Weinreich, R., Hasler, P. H., Novak-Hofer, I., and Schubiger, P. A. (1999) [Br-76]bromodeoxyuridine, a Potential Tracer for the Measurement of Cell Proliferation by Positron Emission Tomography, in vitro and in vivo Studies in Mice. *Nucl. Med. Biol.* 26, 673–679.
  - (8) Bennett, J. J., Tjuvajev, J., Johnson, P., Doubrovin, M., Akhurst, T., Malholtra, S., Hackman, T., Balatoni, J., Finn, R., Larson, S. M., Federoff, H., Blasberg, R., and Fong, Y. M. (2001) Positron Emission Tomography Imaging for Herpes Virus Infection: Implications for Oncolytic Viral Treatments of Cancer. *Nat. Med.* 7, 861–865.
  - (9) Anderson, C. J., Jones, L. A., Bass, L. A., Sherman, E. L. C., McCarthy, D. W., Cutler, P. D., Lanahan, M. V., Cristel, M. E., Lewis, J. S., and Schwarz, S. W. (1998) Radiotherapy, Toxicity and Dosimetry of Copper-64-TETA-Octreotide in Tumor-Bearing Rats. *J. Nucl. Med.* 39, 1944–1951.
  - (10) Anderson, C. J., Dehdashti, F., Cutler, P. D., Schwarz, S. W., Laforest, R., Bass, L. A., Lewis, J. S., and McCarthy, D. W. (2001) Copper-64-TETA-octreotide as a PET Imaging Agent for Patients with Neuroendocrine Tumors. *J. Nucl. Med.* 42, 213–221.
  - (11) McCarthy, D. W., Shefer, R. E., Klinkowstein, R. E., Bass, L. A., Margenau, W. H., Cutler, C. S., Anderson, C. J., and Welch, M. J. (1997) The Efficient Production of High Specific Activity Cu-64 Using a Biomedical Cyclotron. *Nucl. Med. Biol.* 24, 35–43.
  - (12) McCarthy, D. W., Bass, L. A., Cutler, P. D., Shefer, R. E., Klinkowstein, R. E., Herrero, P., Lewis, J. S., Cutler, C. S., Anderson, C. J., and Welch, M. J. (1999) High Purity Production and Potential Applications of Copper-60 and Copper-61. *Nucl. Med. Biol.* 26, 351–358.
  - (13) Rosewicz, S., Vogt, D., Harth, N., Grund, C., Franke, W. W., Ruppert, S., Schweitzer, E., Riecken, E.-O., and Wiedenman, B. (1992) An Amphicine Pancreatic Cell Line: AR42J Cells Combine Exocrine and Neuroendocrine Properties. *Eur. J. Cell Biol.* 59, 80–91.
  - (14) Christophe, J. (1994) Pancreatic Tumoral Cell Line AR42J: An Amphicine Model. *Am. J. Physiol. (Gastrointest. Liver Physiol.)* 266(29), G963-G971.
  - (15) Anderson, C. J., Pajeau, T. S., Edwards, W. B., Sherman, E. L. C., Rogers, B. E., and Welch, M. J. (1995) In vitro and in vivo Evaluation of Copper-64-Labeled Octreotide Conjugates. *J. Nucl. Med.* 36, 2315–2325.
  - (16) Lewis, J. S., Laforest, R., Lewis, M. R., and Anderson, C. J. (2000) Comparative Dosimetry of Copper-64 and Yttrium-90-labeled Somatostatin Analogues in a Tumor-bearing Rat Model. *Cancer Biother. Radiopharm.* 15, 593–604.
  - (17) Breeman, W. A. P., Hofland, L. J., Bakker, W. H., van der Pluijm, M., van Koetsveld, P. M., de Jong, M., Setyono-Han, B., Kwekkeboom, D. J., Visser, T. J., Lamberts, S. W. J., and Krenning, E. P. (1993) Radioiodinated Somatostatin Analogue RC-160: Preparation, Biological Activity, in vivo Application in Rats and Comparison with [<sup>123</sup>I-Tyr<sup>3</sup>]octreotide. *Eur. J. Nucl. Med.* 20, 1089–1094.
  - (18) Foulon, C. F., Reist, C. J., Bigner, D. D., and Zalutsky, M. R. (2000) Radioiodination via D-amino Acid Peptide Enhances Cellular Retention and Tumor Xenograft Targeting of an Internalizing Anti-epidermal Growth Factor Receptor Variant III Monoclonal Antibody. *Cancer Res.* 60, 4453–4460.
  - (19) Lewis, J. S., Srinivasan, A., Schmidt, M. A., and Anderson, C. J. (1998) In vitro and in vivo Evaluation of <sup>64</sup>Cu-TETA-Tyr<sup>3</sup>-Octreotate. A New Somatostatin Analogues with Improved Target Tissue Uptake. *Nucl. Med. Biol.* 26, 267–273.
  - (20) Cherry, S. R., Shao, Y., Silverman, R. W., Meadors, K., Siegel, S., Chatzioannou, A., Young, J. W., Jones, W. F., Moyers, J. C., Newport, D., Boutenouchet, A., Farquhar, T. H., Andreaco, M., Paulus, M. J., Binkley, D. M., Nutt, R., and Phelps, M. E. (1997) MicroPET: a High-Resolution PET Scanner for Imaging Small Animals. *IEEE Trans. Nucl. Sci.* 44, 1161–1166.
  - (21) Bass, L. A., Wang, M., Welch, M. J., and Anderson, C. J. (2000) In vivo Transchelation of Copper-64 from TETA-octreotide to Superoxide Dismutase in Rat Liver. *Bioconjugate Chem.* 11, 527–532.
  - (22) Sun, X., Wuest, M., Weisman, G. R., Wong, E. H., Reed, D. P., Boswell, C. A., Motekaitis, R., Martell, A. E., Welch, M. J., and Anderson, C. J. (2002) Radiolabeling and in vivo Behavior of Copper-64-labeled Cross-Bridged Cyclam Ligands. *J. Med. Chem.* 45, 469–477.
  - (23) Lewis, J. S., Wang, M., Laforest, R., Wang, F., Erion, J. L., Bugaj, J. E., Srinivasan, A., and Anderson, C. J. (2001) Toxicity and Dosimetry of <sup>177</sup>Lu-DOTA-Y3-octreotate in a Rat Model. *Int. J. Cancer* 94, 873–877.

BC015590K